Final Report

National Aeronautics and SpaceAdministration
Research Grant NAG 13-40

"Detection of Metallic Compounds in Rocket Plumes Using Ion Probes"

January 5, 1998

Submitted by

Robert W. Dunn
Associate Professor
Department of Physics
Hendrix College
Conway, Arkansas 72032

FINAL REPORT

National Aeronautics and Space Administration

Research Grant NAG 13-40

"Detection of Metallic Compounds in Rocket Plumes Using Ion Probes."

Introduction

Assuming non-Metalized fuel, the presence of metallic ions in the plume of a rocket may indicate engine distress and could be a precursor to failure. This project is an experimental investigation of the extent to which the presence of metallic compounds can be observed in a rocket plume using ion detectors. The tests were performed on lab scale hybrid rockets constructed by Keith Hudson's group at the University of Arkansas at Little Rock (UALR)[1] and some demonstration grains at Hendrix College in Conway, Arkansas. The metal was introduced in two ways. In the first method, the hydroxyl-terminated polybutadiene (HTPB) fuel grains were seeded with powered metal. In the second approach, the fuel grain was allowed to burn into a solid strips of metal imbedded in the HTPB.

Two methods for detecting ions are used. The first uses ion probes. Ion probes will respond to charges that collide with it and to a lesser extent charges moving in its near vicinity. Intrusion of the probe into the rocket plume often causes them to degrade. Although less sensitive, the second approach is non-intrusive. An insulated short Gaussian cylindrical encloses, but does not touch, the plume. A net charge imbalance in the plume will induce measurable currents in the cylinder.

The specific questions examined in this study are as follows:

1. How reliably can a probe detect metallic compounds in a hybrid rocket plume?
2. How reliably can the Gaussian cylinder detect metallic compounds in a hybrid rocket plume?
3. What are the charging mechanisms that allow the metallic ions to be observed?
4. Do different metallic species have a unique signal? That is, can different species be identified?
5. Is there a difference between seeding the fuel grain with metallic powder and imbedding solid metal in the fuel grain?

Background

Measurements on ionized gases using probes started at least as early as the 1920's. Loeb[2] provides an extremely well documented discussion of these studies. Much of the early interest was created by the emerging vacuum tube technology. Ionizing processes are amazingly varied and complex. The pneumatic transport of particulate material almost always charges the particles, often creating electric fields high enough to initiate discharges. Particles traveling in an ionized gas of one predominant sign will acquire a non-zero charge. Contact between two metals with different work functions can produce a transfer of electrons. This process results in the metals having opposite charges. Frictional contact between insulators can also result in particle charging. Liquid droplets created by a nozzle are normally charged. If the temperature is high enough, thermionic emission of electrons can leave particles with a positive charge. An expanded discussion of these macroscopic particle charging mechanisms is provided by Hendricks[3]. A survey of ionization in flames including rocket plumes is provided by Gaydon and Wolfhard[4]. In flames, ions of both charges and electrons can be produced by a combination of chemical reactions and thermal ionization. They discuss studies for hydrocarbon-oxygen rockets that show chemical ionization is particularly important if hydrocarbon fragments remain in the exhaust. Metallic impurities are cited as significant factors in transporting charge in a rocket plume because the ions resulting from chemical ionization transfer to the metal atoms, thus slowing their recombination rate.

In the 1970's a series of studies were conducted at Wright-Patterson AFB on the detection of metallic particles in jet engine exhausts[5]. The impetus for this study was the catastrophic failure of a compressor blade while the engine was in a test stand. Prior to the failure, strip chart recorder traces from ion probes being used in a combustion study started showing large random spikes. It was concluded these spikes were caused by metallic particles coming from the compressor blade prior to its failure. In subsequent experiments, it was shown that metal particles ingested or created within a jet engine created detectable charges in the exhaust. The exact charging mechanism remained elusive. A study by McDonnell Douglas Research Laboratories, St. Louis, Missouri[6] concluded that the potentials required to produce

those spikes where likely due to clouds of positive electrical charge convected with the exhaust gas. The mechanisms producing the charge was not totally understood.

Experimental Approach

This study is an attempt to apply the experimental techniques developed on jet engine to hybrid rockets. Two difficulties were implicit from the start. Electrostatic charging is often hard to quantify due to the tremendous number of variables affecting the process, and the use of ion probes in a high temperature environment is difficult due to the potential for probe degradation. Small hybrid rockets were selected for this project due to their relative safety and ease of introducing metal. Grains fired at Hendrix College without a nozzle were used to optimize the electronics. Figure 1 shows a diagram of the cylindrical rocket. Powdered metal simulating breakdown in the fuel or oxidant path was introduced by mixing it with the HTPB prior to casting the fuel grain. The powdered metal ranged from 4 to 7 microns in size. By pouring alternate layers of pure HTPB and seeded HTPB in a fuel grain, the effect of introducing metal ions can be studied in a single firing To simulate the effect of burning into the rocket motor, solid pieces of metal were embedded in the fuel. A disadvantage of hybrid rockets for ion studies is the amount of partially burned fuel that is expelled in the plume[7]. These fuel fragments are usually charged and consequently produce responses in the detectors. The igniter uses an exploding wire that injects metallic ions at the start of every run. To eliminate this contamination care had to be exercised to insure sufficient HTPB was burned to clear the rocket before introducing the test metals. Despite their tendency to oxidize, tungsten rods were used as the probes. When the probe was close to the nozzle, the rod became red hot and quickly eroded. To preserve the physical integrity of the rods and to guard against false signals the probe had to be located approximately 62 cm from the nozzle. This helped prevent thermionic emission from the tungsten and prevented false signals due to erosion of the rod. However, the location probably limited the probe's effectiveness, since significant ion recombination is likely to have occurred during transit. By the time the plume gases reach the probe, the temperature has significantly decreased and air has mixed with the combustion products. It was anticipated that the metal would be essentially vaporized when it reached the probe.

However, the data suggests a large particulate content. In fact, much of the charge detected by the probe is apparently carried by particulates. In studies using aluminized fuels in hybrid rockets Lips[8] reports aluminum particles with only partial combustion in the plume. He ascribed the lack of complete combustion to the formation of an aluminum oxide coating around the particles. Since the rocket was in a horizontal configuration, the location of the probe in the plume proved to be important. Locating the probe in a horizontal configuration above the center line of the nozzle greatly reduced the amount of charge detected. Due to the drop experienced by the particulate material between the nozzle and the probe, the best results were obtained when the probe crossed the plume vertically. The end of the rod near the floor extended about 15 cm below the center line of the rocket. When probes are used to measure phenomenon such as electron density, they are normally given an electrical bias. In this experiment no advantages were noted from using an external bias. Therefore, to keep the experiment as simple as possible, the potential was developed across a resistor connecting the probe and the rocket frame. A cylindrical Gaussian surface was used to measure the net charge in the plume. A charge moving in the plume will induce an image charge in a nearby conducting surface. To insure the Gaussian cylinders respond only to induced charges, they were coated with a non-conductive ceramic. External electromagnetic noise picked up by the cylinder was a very serious problem. In some of the initial runs the noise obliterated any useful data The final iteration involved surrounding the plume with two insulated conducting cylinders of approximately the same size and using a sensitive differential amplifier to measure their potential difference. The differential amplifier eliminates electromagnetic noise that is common to the cylinders. Ions emanating from the rocket initially introduce image charges in the first cylinder giving it a different electric potential from the second cylinder. The second cylinder is slightly larger in diameter which accentuates the potential difference due to its reduced sensitivity to the passage of the ions. This approach provides a very sensitive measurement of the net charge moving down the plume. The probe and cylinder as used in this experiment respond to slightly different effects. The probe responds primarily to contact with charged particulates while the cylinder measures the net charge moving in the plume. If the charging process creates an equal number

of positive and negative charges, there must be a spatial separation between the two species to induce image charges in the cylinders. This is probably a major factor in the much greater response of the Gaussian cylinders to the systems without nozzles than to those with nozzles. Without a nozzle the plume exits with a slower velocity and quickly expands. This accelerates the temperature decline, the ion recombination, and the separation of the gaseous material from the particulate material. Figure 2 shows a simplified diagram of the detection system.

Results

Figures 3 and 4 show the response of the probe to consecutive firings of the UALR cylindrical rocket. The first grain was seeded with iron powder and the second with copper powder. The grains were cast in concentric cylindrical layers the inner layer was pure HTPB and the outer layer was 90% HTPB mixed with 10% metal powder by mass. Consequently, the burn started in a layer with only HTPB and moved into one seeded with metal. The results were complicated by the fact the rocket igniter contained a metal wire surrounded by gun powder. When the electrical starter pulse explodes the wire, metal ions are injected into the rocket. Additional ions are probably created by the gun powder. Another complication arose from residual material left over from previous firings. Unless the rocket was cleaned after every firing, residue remained around the nozzle. This was particularly true after firing a grain seeded with metal. This residual material was usually expelled during the next firing In these two runs the probe crossed the plume horizontally and was slightly below the center line of the rocket. The oxygen flow rate was 0.04 lb/sec. The gain on the probe amplifier was 10x and the potential was developed over a 50 kΩ resistor. The first second of the run in figure 3 is dominated by residual material and ions from the igniter. The next five seconds show a few residual particles and the combustion products from the HTPB. After about six seconds the layer seeded with iron powder begins to burn. For the remaining four seconds, the signal is dominated by the powdered iron. In figure 4 the initial five seconds of this run is apparently dominated by igniter wire and the residual iron from the previous grain. The next two seconds shows the combustion products and a few residual particles. The remaining three seconds show the effects of burning the copper powder mixed with the HTPB. A

visual inspection of the fuel grains confirmed the burn had reached the layer seeded with metal. Long runs with straight HTPB eliminated the possibility that the grain geometry was creating these results. After this run the rocket was disassembled and cleaned. An inspection of the nozzle revealed it was covered with specks of copper.

The next two figures show the results of burning into solid pieces of metal embedded in the HTPB. The potential is developed across a 50 kΩ resistor connected between the probe and rocket case. The oxygen flow rate is set at 0.08 lb/sec. Most of the firings in this study used an oxygen flow rate of 0.04 lb/sec. This allowed longer runs without overheating the rocket engine. Figure 5 shows the result of burning into the approximately 20.0 x 0.3 cm edge of an aluminum strip that was embedded in the HTPB. The probe amplifier was set at a grain of 5x. The initial two seconds of the burn were dominated by the residual material. During the rest of the run, aluminum is being melted and expelled though the nozzle. There may have been some overlap between the start of the aluminum burn and the final expulsion of the residual material. However, the increase in amplitude due to the aluminum is clearly evident. A visual examination of the strip revealed that several portions of the strip had been completely burned or melted away during the run. Figure 6 shows the result of burning into the approximately 20.0 x 0.02 cm edge of a stainless steel strip. For this burn, the probe grain was set at 10x. The first two seconds show the residual material and igniter being expelled. The burn reached the stainless steel after about three seconds. In this case, a visual inspection of the stainless steel revealed only some scorching of the metal surface. The strip remained completely intact. Even though a minuscule amount of metal was expelled, it apparently was enough to be detected by the probe. It appears the signal during the last few seconds of the run is due to ions from the stainless steel. However, the possibility that uneven heating of the fuel grain around the metal strip is also injecting HTPB into the plume can not be completely discounted.

The next set of figures were taken on a slab motor instead of the cylindrical rocket. The slab motor was used in an attempt to facilitate the casting of grains with alternate layers of HTPB and HTPB mixed with metal powder. It was also used to study the effect of a different motor geometry. A diagram of the slab motor is shown in Figure 7. The slab motor has a rectangular combustion chamber approximately

50.0 x 7.6 x 5.0 cm. The motor proved unsatisfactory due to pressure spikes. On two occasions, the spikes were severe enough to break the shear pins on the nozzle resulting in the destruction on the probe. Fortunately, the cylinders were large enough for the nozzle to pass through them without making contact. Safety concerns terminated these runs after the second failure. The exact cause of failures is still under investigation. Since the grains where cast in layers, it is possible that part of the top layer delaminated and clogged the nozzle. The Figures 8, 9, and 10 in this section were part of the calibration runs. Consequently, the electronics was not completely optimized. It is not totally clear why the response of the probe contains so many negative excursions. Since some of the pulses saturated the system, the results immediately following may not be accurate. To establish a reliable zero baseline after saturation, the amplifiers need time to recover. A major difference in these graphs, when compared to the cylindrical runs, occurs during the first second after ignition. There is a very limited response to the igniter. The cylindrical rocket has an almost immediate start. It takes the slab motor a second or more to establish its burn. In Figure 8 the top layer of the grain contains powdered iron mixed with HTPB. There is a correlation between the pressure spikes and the response of the probe and Gaussian cylinders. This is the first data taken with the differential amplifier connected between the cylinders as shown in Figure 2. The baseline for the Gaussian cylinders floats upward after the ignition pulses. This could be due to saturation and/or unequal charging of the cylinders. The last response from the Gaussian cylinders occurs after the oxygen has been shut off. To snuff out the flame in the fuel grain, nitrogen is used to purge the system. As long as the normal shut down procedure is followed, a significant response to the nitrogen purge is present. Figure 9 shows the result of aborting a firing in which everything is shut off simultaneously. This run used the same grain that was fired for Figure 8. The rocket operator aborted the firing due to a sudden increase in pressure. The response of both the probe and cylinders to the pressure spikes is clearly shown. Again the probe amplifier is saturated by some of the pulses which makes the subsequent baseline levels unreliable. The reduced response from the Gaussian cylinder after shut down is evident. During this firing, the nozzle was apparently partially clogged by the iron powder fuel mix. Figure 10 shows the detection of a very large particulate, namely

the rocket nozzle. The slow decay follows the shattering of the probe by the nozzle. It is interesting to note that the rapid increase in pressure before failure corresponds to the sharp decrease in charged material being detected by the probe. The nozzle apparently became clogged leading to its failure. There was no metal powder mixed in the grain. Instead, a stainless steel strip was embedded in the HTPB.

For the remaining figures, the cylindrical rocket was used. The figures provide a comparison of the results from the probe and the Gaussian cylinders when the system has not been saturated. The oxygen flow rate is 0.04 lb/sec. The probe amplifier is set at 5x and the cylinder differential amplifier is set at 50x. Figure 11 shows the response to burning into aluminum powder. In this case, the powder was mixed with HTPB and inserted in a hole approximately 1 cm in diameter drilled parallel to the center bore that admits the oxygen. This approach was used because of the time and effort required to cast the grains with uniform concentric fuel layers. In addition, after the problems with the slab motor, there were concerns about delamination. The single large initial spike is the electrical starter pulse. The next positive spikes are associated with the igniter and residual material. There was insufficient time to completely clear the rocket of the residual material before burning into the aluminum. The large positive and negative excursions are associated with burning into the aluminum. Apparently, enough aluminum was suddenly injected into the rocket plume to create the negative excursions. Similar positive and negative excursions were observed in jet exhausts if sufficient quantities of metallic powder was suddenly ingested. The probe responds to both collisions with charges and to near misses. In a collision with a positive ion, electrons are pulled through the resistor onto the probe where they neutralize the ion. This registers as a positive signal on the graph. If a large positive charge passes close to the probe without being neutralized the response is different. Electrons are pulled through the resistor, as before, but when the charge passes beyond the probe the electrons are released from its pull. They now surge back through the resistor. The graph will show a positive response followed by a negative excursion. Usually collisions and near misses occur simultaneously. Normally, the response from the collisions will dominate. Figure 11b shows the response of the Gaussian cylinders to the same firing. The large initial spike is associated with the electrical starter pulse and occurs simultaneously in both

graphs. The positive spikes that follow are created by the residual material. The response containing the first negative excursion is associated with burning into the aluminum. The final large positive and negative signals are the response to the ions expelled by the nitrogen. Apparently, the nitrogen pressure is not sufficient to transport the ions across the 62 cm separation to the probe.

The next two Figures 12 and 13 show burns into solid strips of aluminum and stainless steel. The amount of aluminum released is much greater than that of stainless steel. In these firings, the oxygen flow rate is 0.04 lb/sec. The probe amplifier was set at 10x and the differential amplifier was set at 50x. Figure 12 shows the probe and cylinder response to burning into a strip of aluminum embedded in HTPB. It was toward the end of the run before the burn hit the aluminum. An examination of the nozzle after shut down revealed droplets of solidified aluminum. Figure 13 shows the response to a burn into a strip of stainless steel. Very little response is generated by the Gaussian cylinder as the burn moves into the stainless steel. The probe clearly indicates the presence of positive ions after the transition. Again there is an initial response to the igniter and residual material. The cylinder also strongly responds to the nitrogen purge. The lack of response from the cylinder to burning the stainless steel probably results from the small amount metal liberated. Another possibility is that the mass of the individual stainless steel ions is small. Although chunks of the aluminum strip had melted, an examination of the stainless strip revealed only scorching of the surface. In order to induce image charges in the cylinder, there must be charge separation in the plume. Close to the nozzle, the plume gases may transport positive ions with little mass at nearly the same rate as the electrons and negative ions. If this is case, only limited charge separation will occur, and the Gaussian cylinder may not respond. The residual material observed on the nozzle is generally a coarse mixture of partially burned metal and charred fuel, which is always detected.

The last two figures provide a comparison between burning HTPB and HTPB mixed with finely powdered graphite. The usual response to the igniter wire and residual material is present in both figures, and the probe response is essentially the same in both cases. After the oxidizer shut down, both figures show the cylinder's typical response to the nitrogen purge. However, the Gaussian cylinder's response is

different to the combustion products found in the region between the residual material and the nitrogen purge. Figure 14 shows a three second run into HTPB. After the initial response to the igniter and residual material, the usual lower level combustion product signals are detected until shut down. Figure 15 shows a four second burn using a fuel grain with 99% HTPB and 1% graphite by mass. There are no boundary layers in this grain. The graphite is exposed to the burn from the start. Therefore, any comparisons have to be made between the straight HTPB grain and the grain mixed with graphite. Although the runs for these two figures were not sequential, they were made under the same conditions with identical settings. There is a stronger, but not overwhelming, response to the graphite by the cylinder in Figure 15 than in Figure 14. This is consistent with the previous results, assuming that the graphite is essentially consumed in the combustion process and does not form particulates. Under this scenario, the probe does not detect much of a presence from graphite because no particulates are formed. However, burning the graphite apparently creates additional positive ions. The cylinder responds to the additional positive charge, but the ions either do not reach the probe or recombine in transit. If the graphite powder was coarser and there was incomplete burning, the probe might show a greater response.

Conclusions

The data conclusively demonstrates that ion probes are reliable qualitative detectors of particulate metal in the plume. In every case in which metal was released in the rocket it was detected by the probe. The detection process was complicated by the presence of metal in the igniter. Also there was a tendency for residual metal and charred fuel to coat the nozzle after a firing. Subsequent firings often ejected the residual material for a few seconds after ignition. In addition to metallic compounds, ion probes also respond to other types of charge carriers. In hybrid rockets using HTPB, the metallic ions carried a larger charge than the combustion products or at least they produced a greater response from the probe. Therefore, the metallic ions can be distinguished from the combustion products by comparing the amplitude of the probe's responses. The grains seeded with metallic compounds also produced a larger response in the probe than the grains mixed with

graphite. However, graphite is continually introduced through ablation of the nozzle and the percent of graphite mixed with the grain was low.

The ability to discriminate between metallic species was not demonstrated. It seems plausible that if the physical integrity of the probe could be maintained near the nozzle that additional information would be available. Ion recombination is much less likely near the nozzle than in the region where the probe data was taken. Biasing the probe with an external potential is a technique that might prove advantageous near the nozzle. Whether a unique metallic ion signature could be established, even using an external bias, seems at this point to be highly speculative. The key factor in the detection of metallic ions by the probe is the apparent incomplete burning that results in particle formation. All the metal species used in this study apparently formed particulates. This was demonstrated by the decrease in response to metallic compounds as a horizontal probe was raised above the center line of the rocket. The literature[4] suggests that ion transfer to metallic impurities helps preserve positive charge in the plume, since attachment to the metal slows charge neutralization through ion recombination. All the results in this study support that hypothesis. A variety of processes initially create the ions with chemical ionization being a major contributor.

Optimization of the Gaussian cylinders was more involved due to its high sensitivity to electrical noise. As a consequence, less data is available from the Gaussian cylinders than from the probes. Detection using the cylinders is also limited by the necessity for the positive and negative charges to be spatially separated in the plume. Once they were optimized, the only time a discernible response to metallic ions was not clearly observed was during the burns into the stainless steel strips. In this case, there was probably not enough additional charge in comparison to the combustion ions to be observed. Also, there may have been insufficient charge separation in the plume. The use of external electric fields might increase the charge separation in the plume and consequently enhance the response of the cylinder. The insulating ceramic was not necessary for charge detection, but was included to prevent contact charging. This made observing the formation of image charges easier to identify. The cylinders could be formed from graphite in a manner similar to that used for the nozzle. If they were insulated from the rocket and mounted at the

edge of the plume, the cylinders could then detect charges both by contact and induction.

The metal was detected regardless of whether it originated as powder mixed with the HTPB or by the flame burning into metal embedded in the fuel. Pieces of the aluminum and the copper strips were burned or melted away. The stainless steel strip was just scorched, suggesting few metallic ions were created.

Acknowledgments

This project would not have been possible without the assistance of Keith Hudson and his group at the University of Arkansas at Little Rock. As the hybrid rocket operator, Ann Wright was indispensable.

References

1. Shanks, R.B. and Hudson, M.K., "The Design and Construction of a Labscale Hybrid Rocket Facility for Spectroscopy Studies," AIAA Paper No. 94-3016, June 1994.

2. Loeb, L.B., *Basic Processes of Gaseous Electronics* (University of California Press, Los Angeles, CA, 1955).

3. Hendricks, C.D., "Charging Macroscopic Particles." *Electrostatics and Its Applications*, ed. A.D. Moore (John Wiley and Sons, New York, 1973).

4. Gaydon, A.G. and Wolfhard, H.G., *Flames* (Chapman and Hall Ltd, London, 1970).

5. Couch, R.P., et al., "Sensing Incipient Engine Failure." Progress in Astronautics and Aeronautics, 34:515-529 (1972).

   Hill, G.E., "Imminent Engine Failure Probe Investigation." AFAPL TR-74-30. Wright-Patterson Air Force Base, Ohio: Air Force Aero Propulsion Laboratory, 1974.

   Mitchell, D.A. and Mario S., "Evaluation of an Electrostatic Probe Technique for Detection of Turbine Engine Gas Path Distress, Comprehensive Summary Report." AFAPL TR-74-96. Wright-Patterson Air Force Base, Ohio: Air Force Aero Propulsion Laboratory, 1975.

   Mitchell, D.A. and Mario S., "Evaluation of an Electrostatic Probe Technique for Detection of Particles Emitted During Turbine Engine Distress." AFAPL TR-74-71. Wright-Patterson Air Force Base, Ohio: Air Force Aero Propulsion Laboratory, November 1974.

6. Sajber, et al., "Evaluation of Experiments Using Electrostatic Probes to Detect Imminent Failure of Jet-Engine Gas-Path Components," AFFDL TR-75-74. Wright-Patterson AFB, Ohio: Air Force Flight Dynamics Laboratory, July, 1975.

7. Yi, J., et al., "Hybrid Combustion with Metallized Fuels," AIAA Paper No. 93-2410, June 1993.

8. Lips, H.R., "Experimental Investigation on Hybrid Rocket Engines Using Highly Aluminized Fuels," AIAA Paper No. 76-640, July 1976.

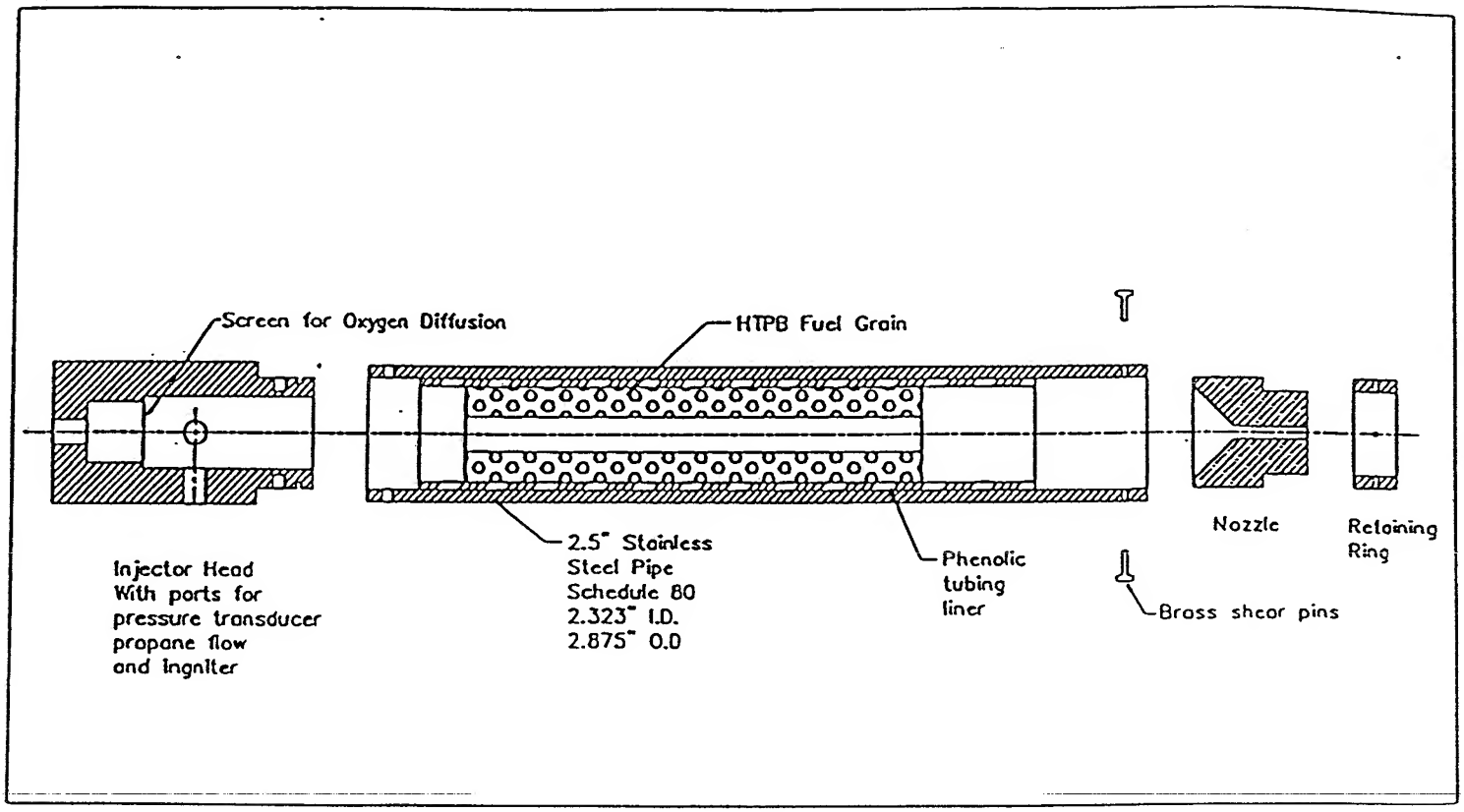

Fig. 1 This figure shows the layout of the 44 cm UALR cylindrical labscale hybrid rocket motor. It operates on gaseous oxygen and hydroxyl-terminated polybutadiene (HTPB) solid fuel. The fuel grain is 5 cm in diameter and 25 cm long. The central port of the fuel grain is 2 cm in diameter. In the firing sequence the oxidizer flow is initially established. Two seconds later the propane flow is initiated. One second after the propane flow begins, the igniter is fired. After the preprogrammed firing duration, the oxidizer flow is shut off. The combustion chamber is them purged with nitrogen [Taken from Shanks and Hudson[1]]

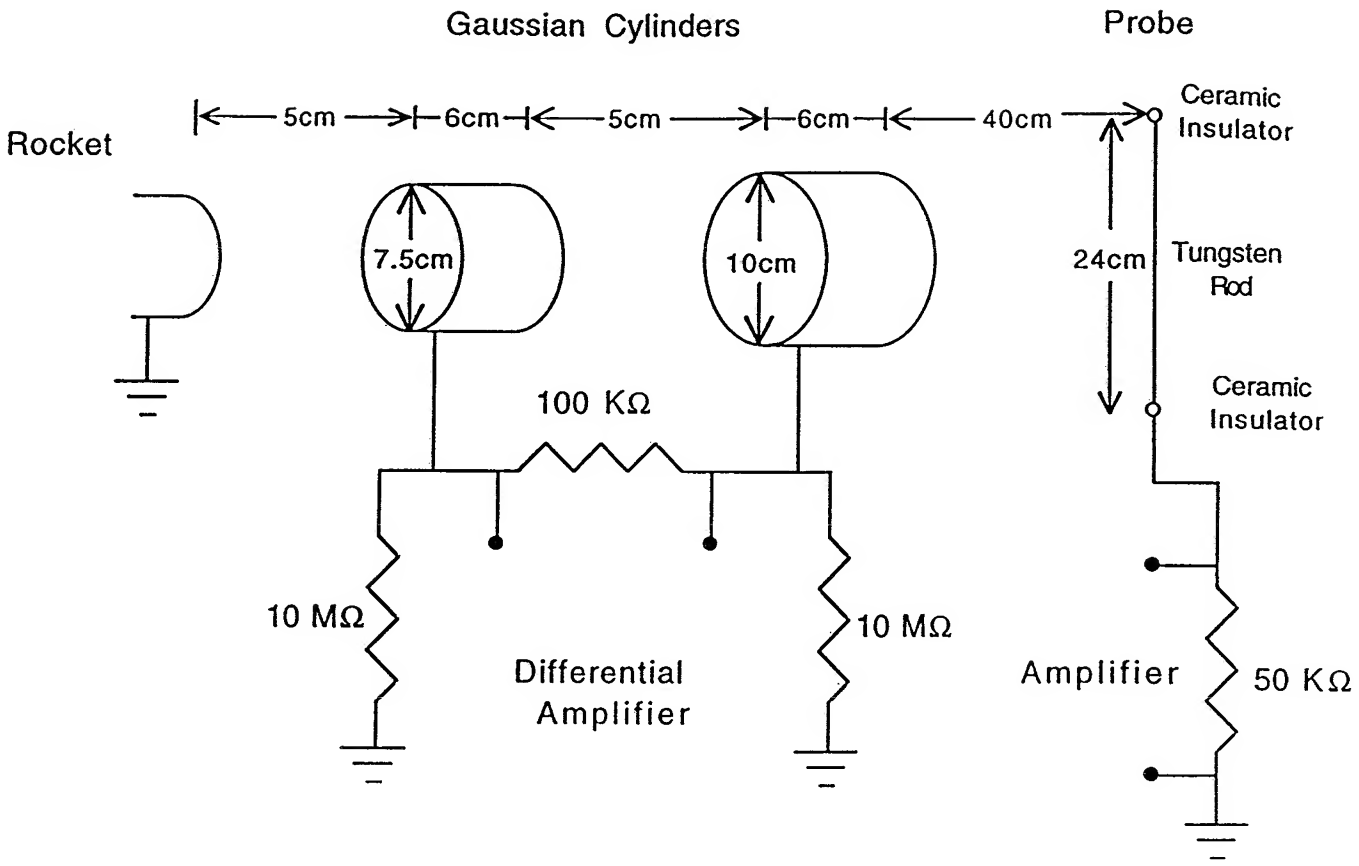

Fig. 2 This figure is a diagram of the ion detectors. The potential difference between the two Gaussian cylinders is developed across a 100 kΩ resistor. The 10 MΩ resistors are used to keep the potential of the cylinders equal to that of the rocket except when ions are present in the rocket plume. The second cylinder is slightly larger than the first one. This makes the first cylinder more sensitive to the passage of ions. The size difference does not preclude the differential amplifier from canceling electrical noise. When an ion enters the first cylinder it induces an image charge that creates a potential difference between the cylinders. The ion then passes through the second cylinder. The polarity of the potential difference reverses but the second cylinder is less sensitive because of its larger diameter. Therefore the first cylinder tends to dominate the response. The potential for the probe is developed over a 50 kΩ resistor, that is connected between the tungsten rod and the rocket frame. The probe will respond to charges that collide with it or to charges that pass in its near vicinity. As positive charges approach the probe electrons flow through the resistor onto the tungsten rod. This registers as a positive spike. If there is a collision the charge is neutralized. If the charge passes without hitting the probe the electrons eventually flow back across the resistor in the opposite directions creating a negative spike.

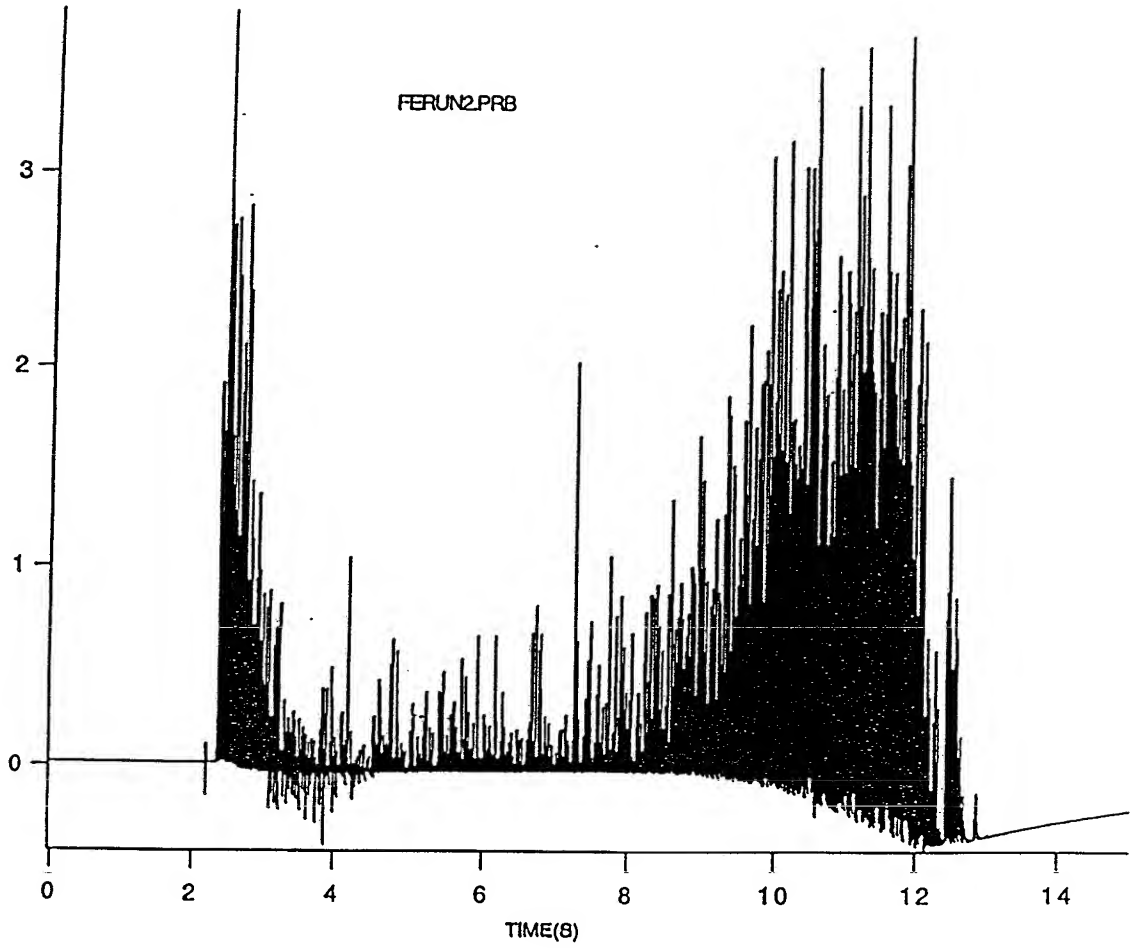

Fig. 3 This grain was poured in two layers. The first layer contained HTPB. The second layer contained HTPB mixed with iron powder in a 9 to 1 mass ratio. The powder is approximately 4 microns in diameter. The large amplitude spikes for the first second are a combination of the exploding igniter wire and the gunpowder coating. Residual metal and charred fuel left on the nozzle from previous runs also contribute to these spikes. The lower amplitude spikes lasting for the next six seconds are the combustion products from the HTPB. There are still a few spikes from the residual material during this interval. The final four seconds result from burning into the layer containing the iron powder. The oxygen flow rate was 0.4 lb/sec and the probe gain was 10x.

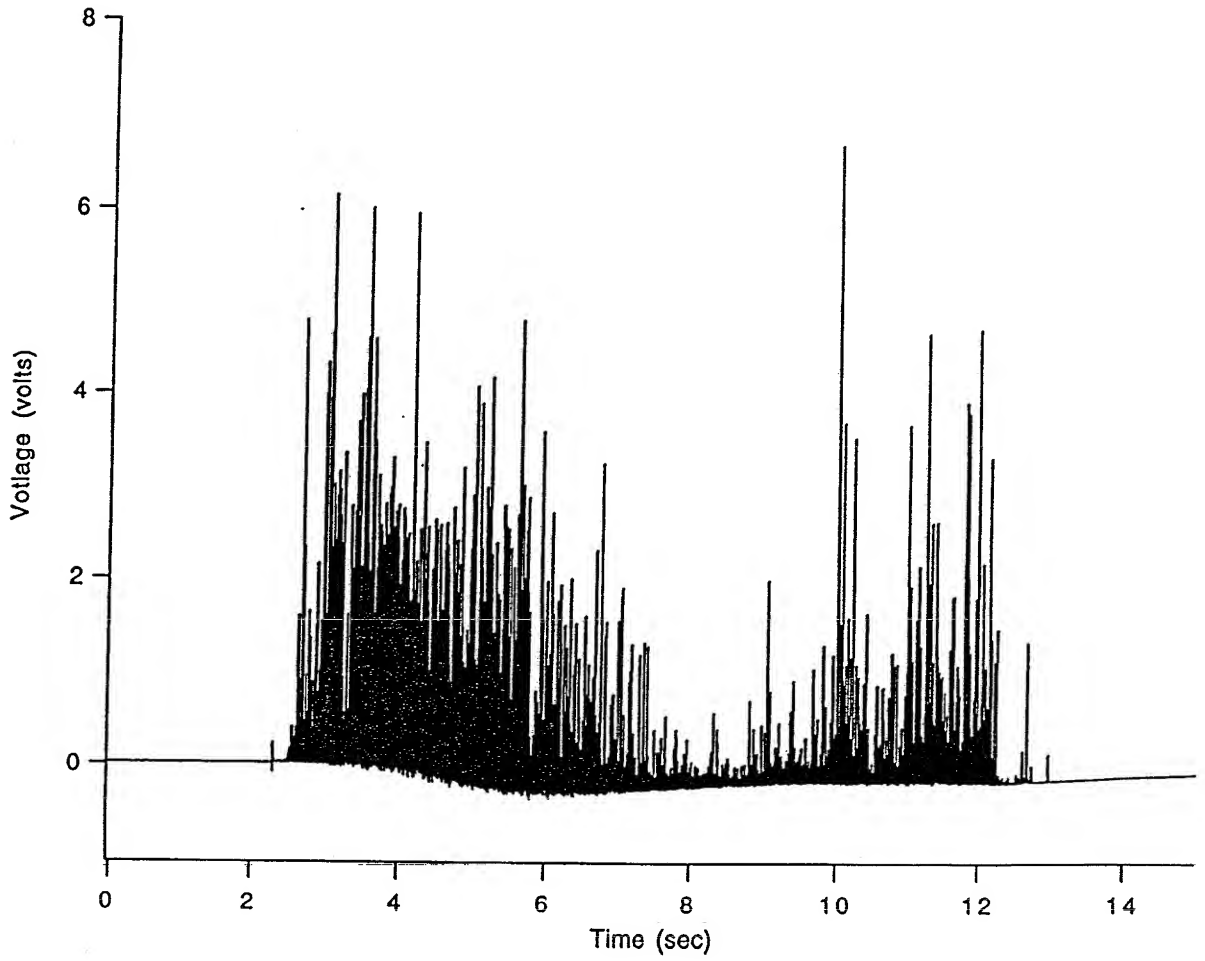

Fig. 4 This grain was poured in two layers. The first layer contained HTPB. The second layer contained HTPB mixed with copper powder in a 9 to 1 mass ratio. The powder is approximately 7 microns in diameter. The large amplitude spikes for the first five seconds are a combination of the exploding igniter wire and the gunpowder coating. Residual metal and charred fuel left on the nozzle from previous runs also contribute to these spikes. The lower amplitude spikes lasting for the next three seconds are the combustion products from the HTPB. There are still a few spikes from the residual material during this interval. The final four seconds result from burning into the layer containing the copper powder. The oxygen flow rate was 0.4 lb/sec and the probe gain was 10x. A comparison with Figure 3 shows the effect of the iron powder embedded in the nozzle. In this run, it took about four seconds longer to clear the residual material. After this run the rocket was disassembled for cleaning. A visual examination of the nozzle revealed that copper specks covered its interior surface.

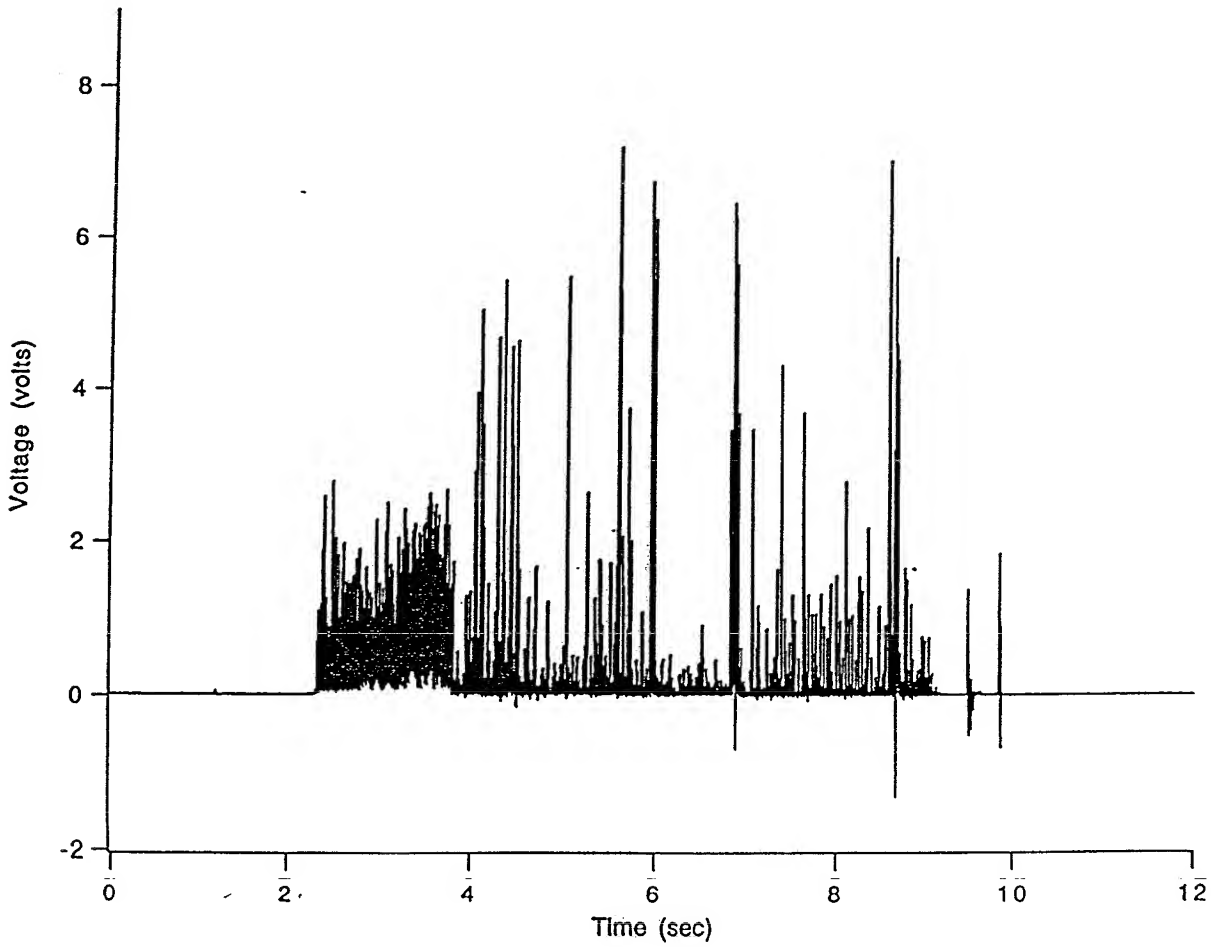

Fig. 5 An aluminum strip was embedded in this grain. The spikes initially lasting for about two seconds were caused by the igniter and the residual material left in the rocket. A miscalculation of the regression rate resulted in the aluminum being burned before the residual material was completely expelled. However, the presence of the aluminum is clearly shown by the large amplitude spikes that started about two seconds into the run. The oxygen flow rate is 0.08 lb/sec which was one of the highest rates used in these experiments. The probe gain was down to 5x. The aluminum would have saturated the amplifiers if the gain had remained at 10x as in Figures 3 and 4. Pieces of the aluminum were completely consumed during the run.

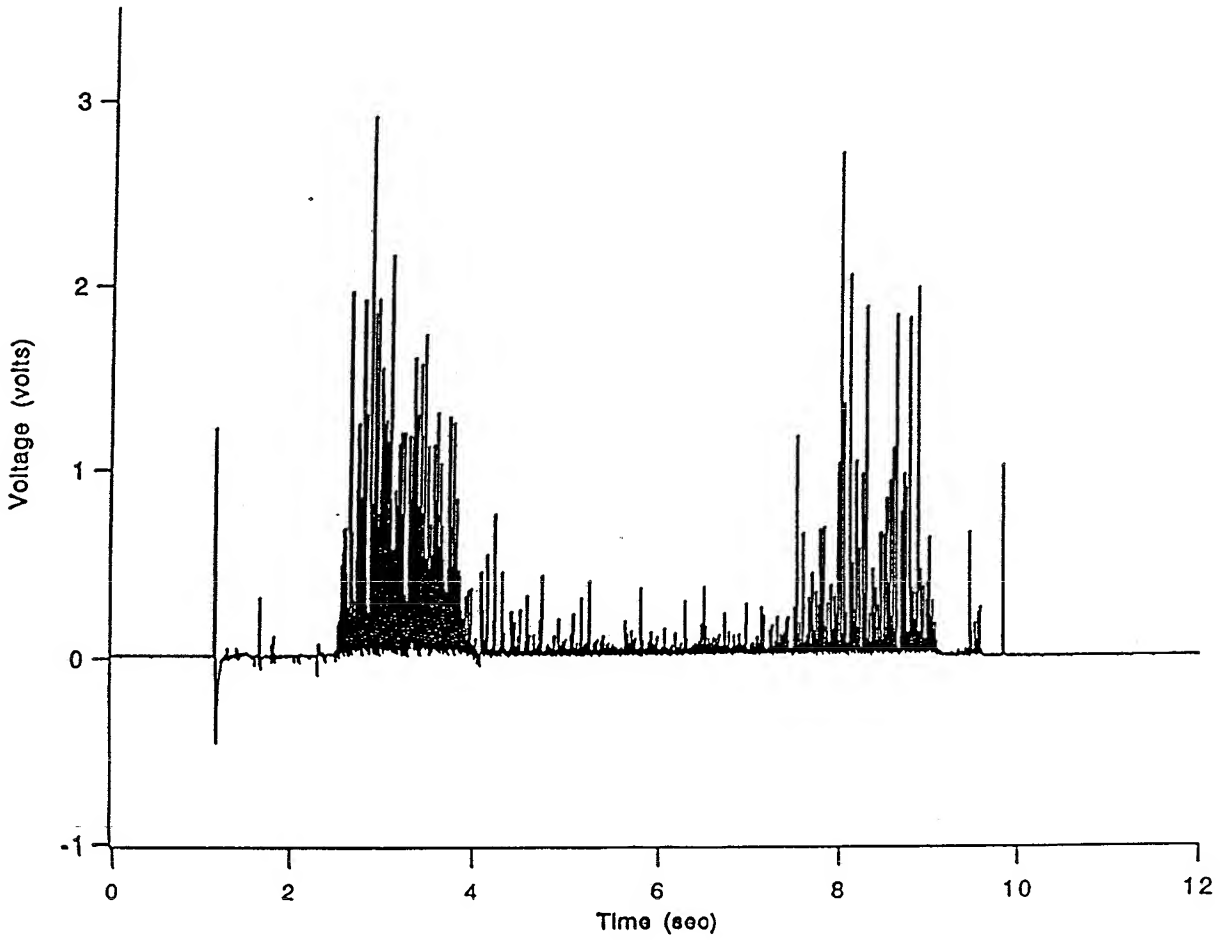

Fig. 6 A stainless steel strip was embedded in this grain. The initial nearly two seconds of the run is dominated by the igniter and residual material. The next four seconds show the HTPB combustion products. The remainder of the run shows the effect after burning into the stainless steel. The oxygen flow rate was 0.8 lb/sec and the probe gain was set at 10x. Although it is hard to make reliable comparisons between runs, the response to the stainless steel appears to be about 80% less than the response to aluminum, when the difference in amplification is included. The stainless steel strip was still intact. Its surface appeared scorched but a minimal amount of metal was ablated.

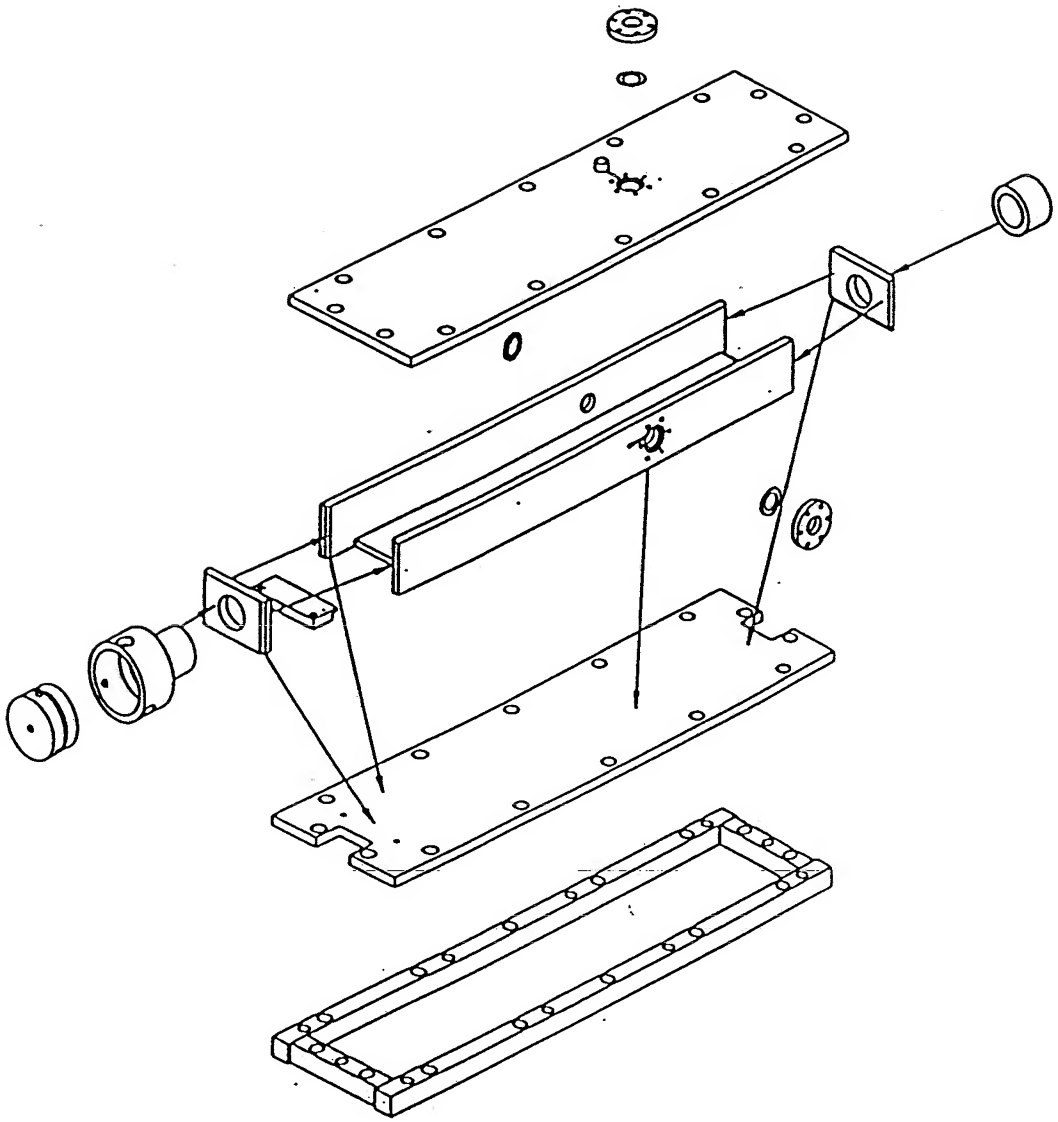

Fig. 7 The slab motor is shown in this figure. The combustion chamber is approximately 50.0 x 7.6 x 5.0 cm. The pressure and temperature were lower in the slab motor than in the cylindrical motor. Consequently less material is ejected per second during normal operation. The slab motor was much more sluggish in establishing a steady burn than the cylindrical motor. The motor eventually proved unsatisfactory due to pressure spikes, that finally broke the shear pins holding the nozzle.

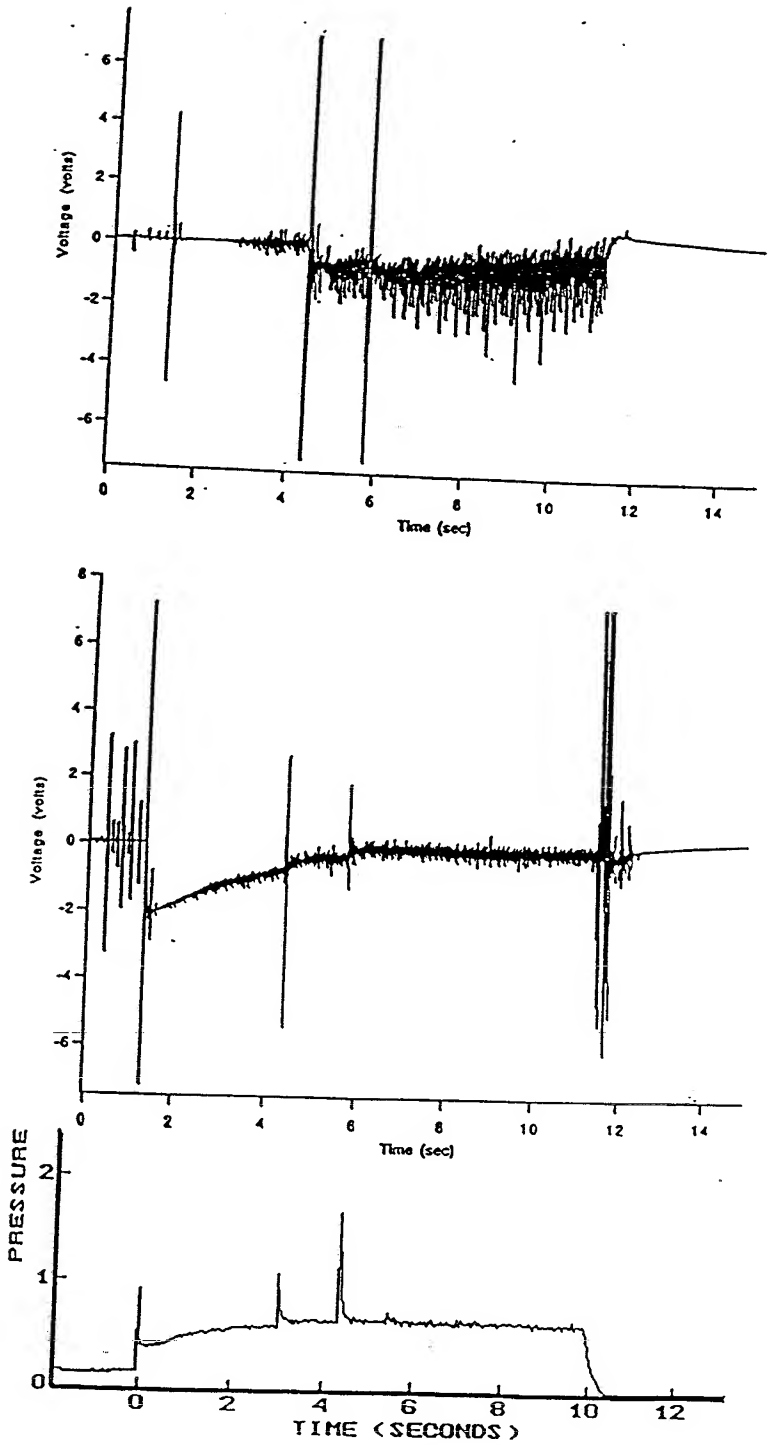

Fig. 8 The slab motor grain for this run was poured in two layers. The top layer was mixed with iron powder and HTPB. The bottom layer was HTPB. The transition was not reached during this run. In the top graph the probe amplifier is saturated by the material ejected during the pressure spikes. The second graph shows the response of the Gaussian cylinders. Noise from the solenoids opening the valves prior to the igniter pulse is evident in the top graphs. The last signal in the second graph occurred after the oxidizer was shut off and was a response to the nitrogen purge. The third graph is the pressure trace taken by the computer controlling the rocket.

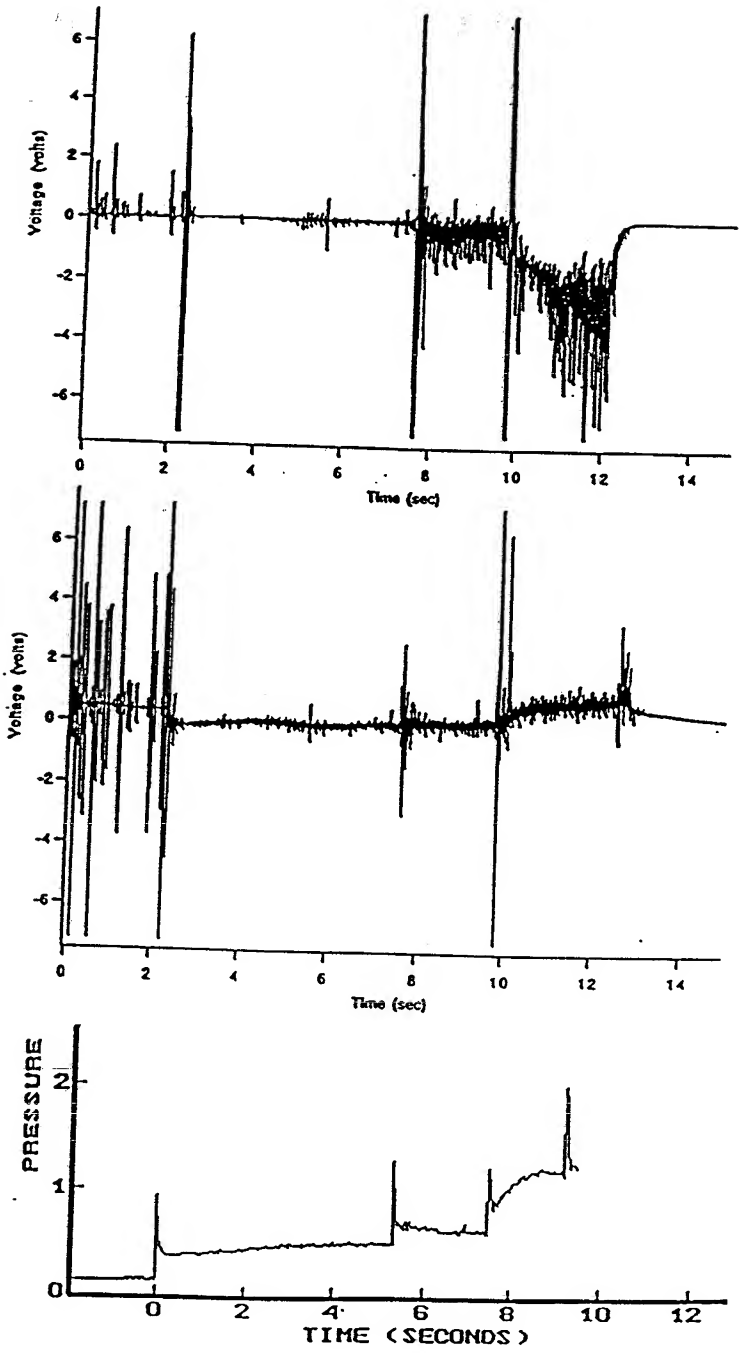

Fig. 9 For this figure, the grain from Figure 8 was again burned. The transition between the HTPB metal mix and the HTPB was still not reached. The initial response to the igniter and residual material is much less than the response from the cylindrical motor. This may be due to the length of time it takes to get the burn started. This run was aborted after the third spike. The response of the cylinders, after the oxidizer is cut off, is considerable reduced because there is no nitrogen purge. The probe amplifier in the top graph is saturated. The data following saturation is unreliable, since the amplifiers require a certain period of time to recover. The noise associated with the solenoids opening the valves prior to ignition is evident in the upper graphs.

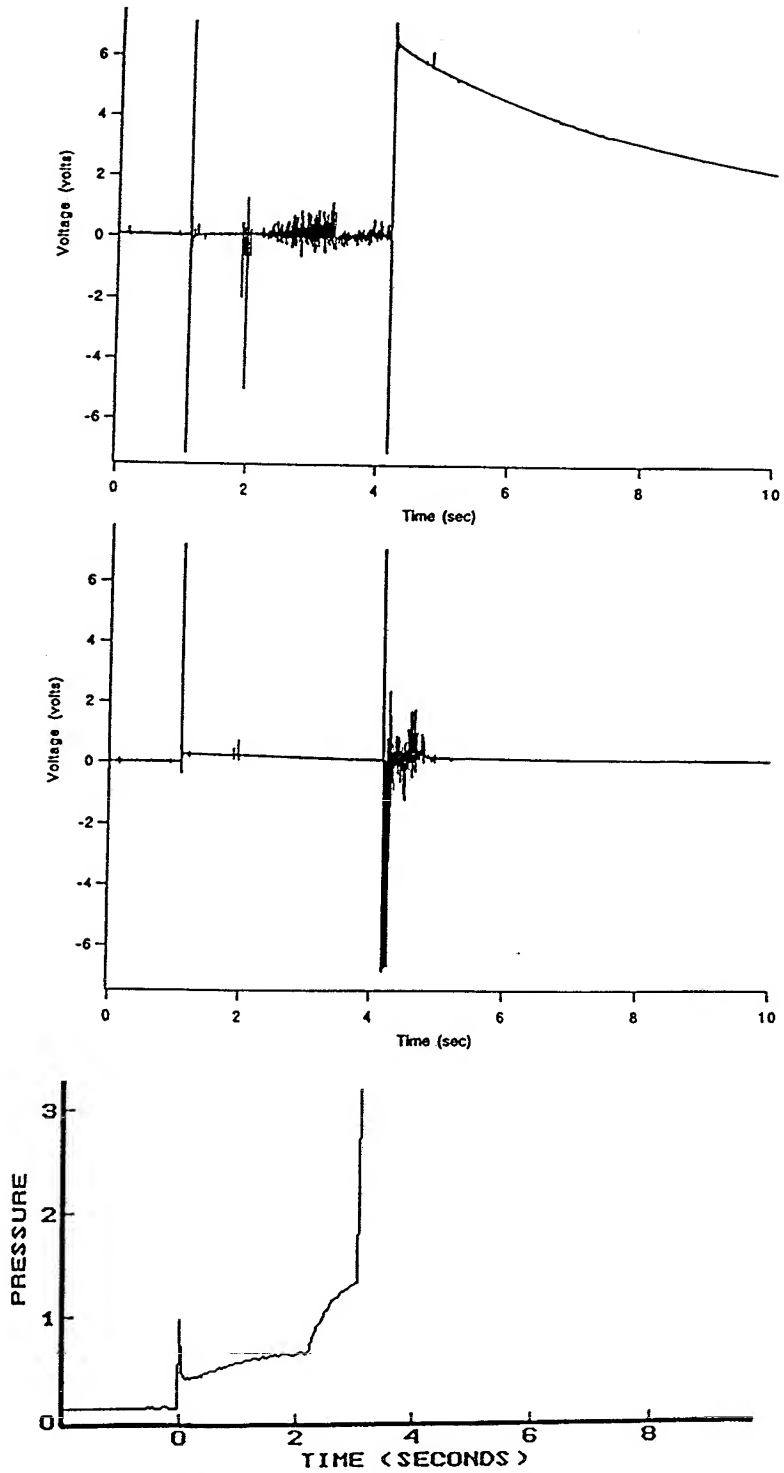

Fig. 10 A strip of stainless steel was embedded in this grain. During the run over pressure broke the shear pins holding the nozzle. An examination of the top graph shows a sharp drop in the amount of charged material being detected about two seconds after the ignition pulse. At the same time the bottom graph shows the pressure beginning to rapidly increase. At about three seconds after ignition, the rocket failed and the probe was destroyed. The second graph shows the spike associated with the passage of the nozzle through the cylinders. Apparently the nozzle was partially obstructed leading to the over pressure. A visual examination of the grain indicated the burn had contacted the stainless steel before the rocket failed. Uneven heating may have caused some HTPB to spall off and obstruct the nozzle.

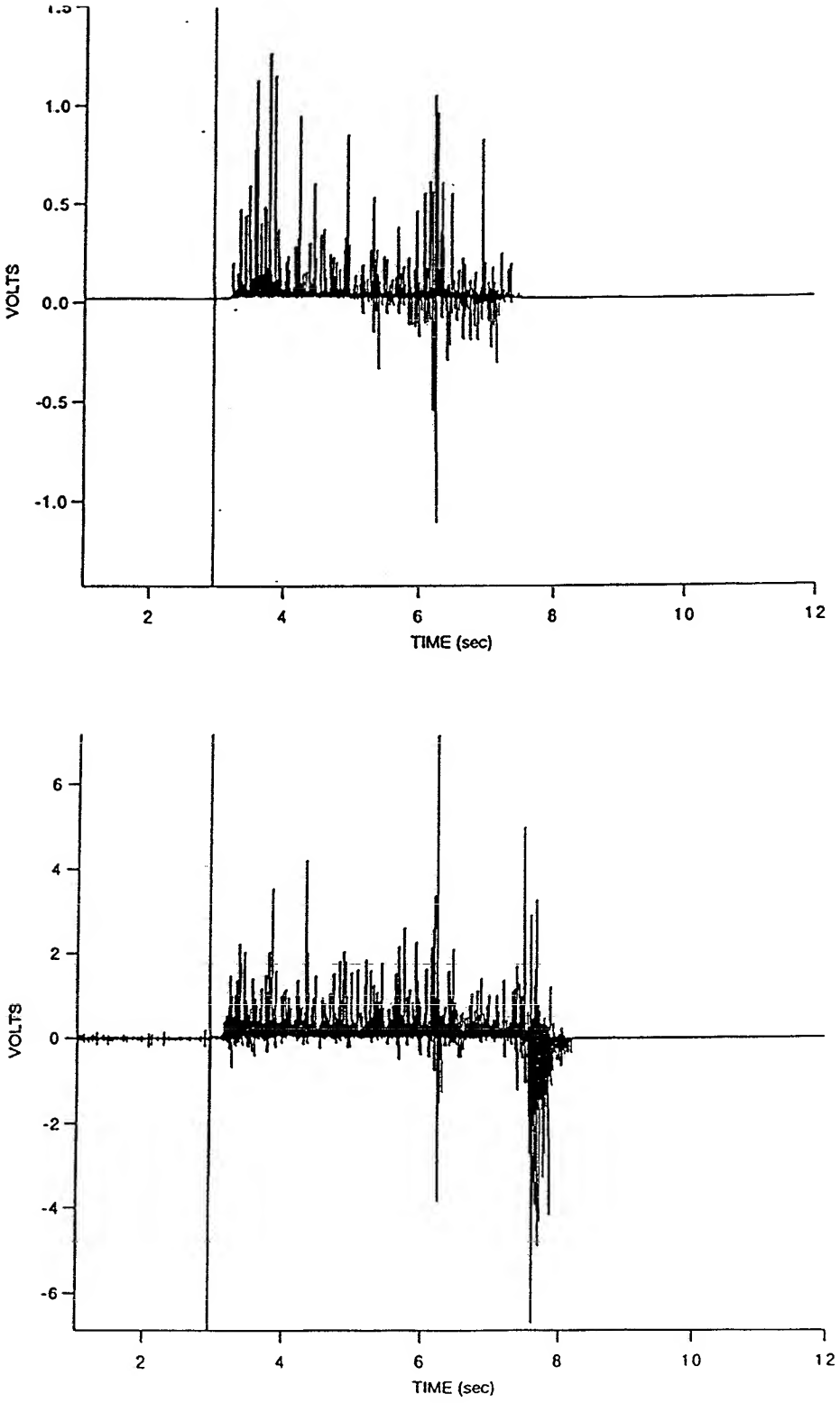

Fig. 11 The cylindrical rocket is used to show the response of the probe and Gaussian cylinders to a transition into powdered aluminum mixed with HTPB. The HTPB mix was placed in a hole 1 cm in diameter drilled parallel to the center bore of the fuel grain. The transition occurred a little over three seconds after the igniter pulse. The response of the Gaussian cylinders is in the bottom graph. The oxidizer is turned off four seconds after the starter pulse. The final large response is created by the nitrogen purge.

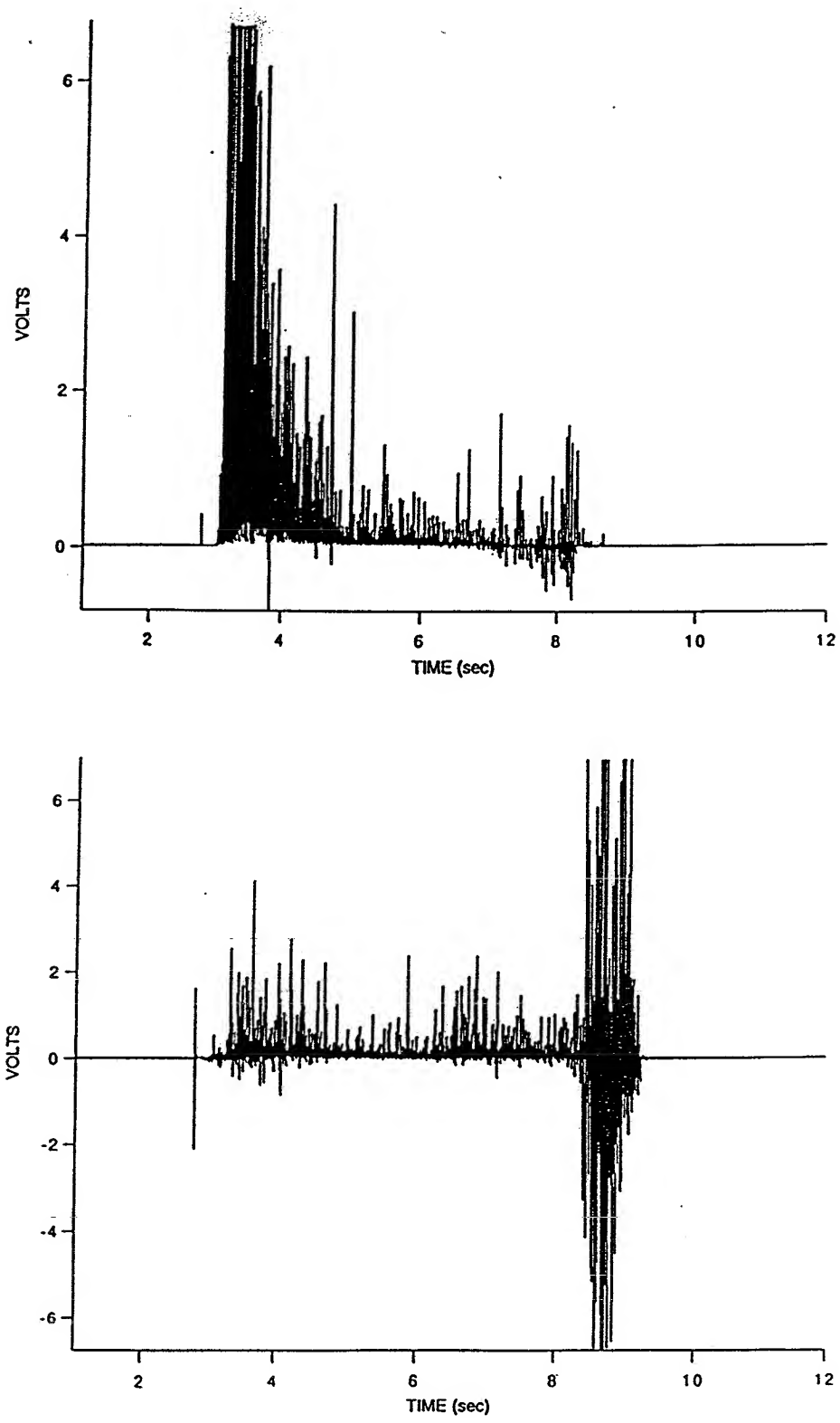

Fig. 12 A transition into a solid strip of aluminum is shown in this figure. The transition occurred near the end of the run and less aluminum was burned than in Figure 5. Also the oxygen flow rate was only half the rate used in Figure 5. Part of the response from the cylinders in the bottom graph merges with the signals from the nitrogen purge. The limited response when compared to Figure 5 is probably caused by the reduced oxygen flow rate.

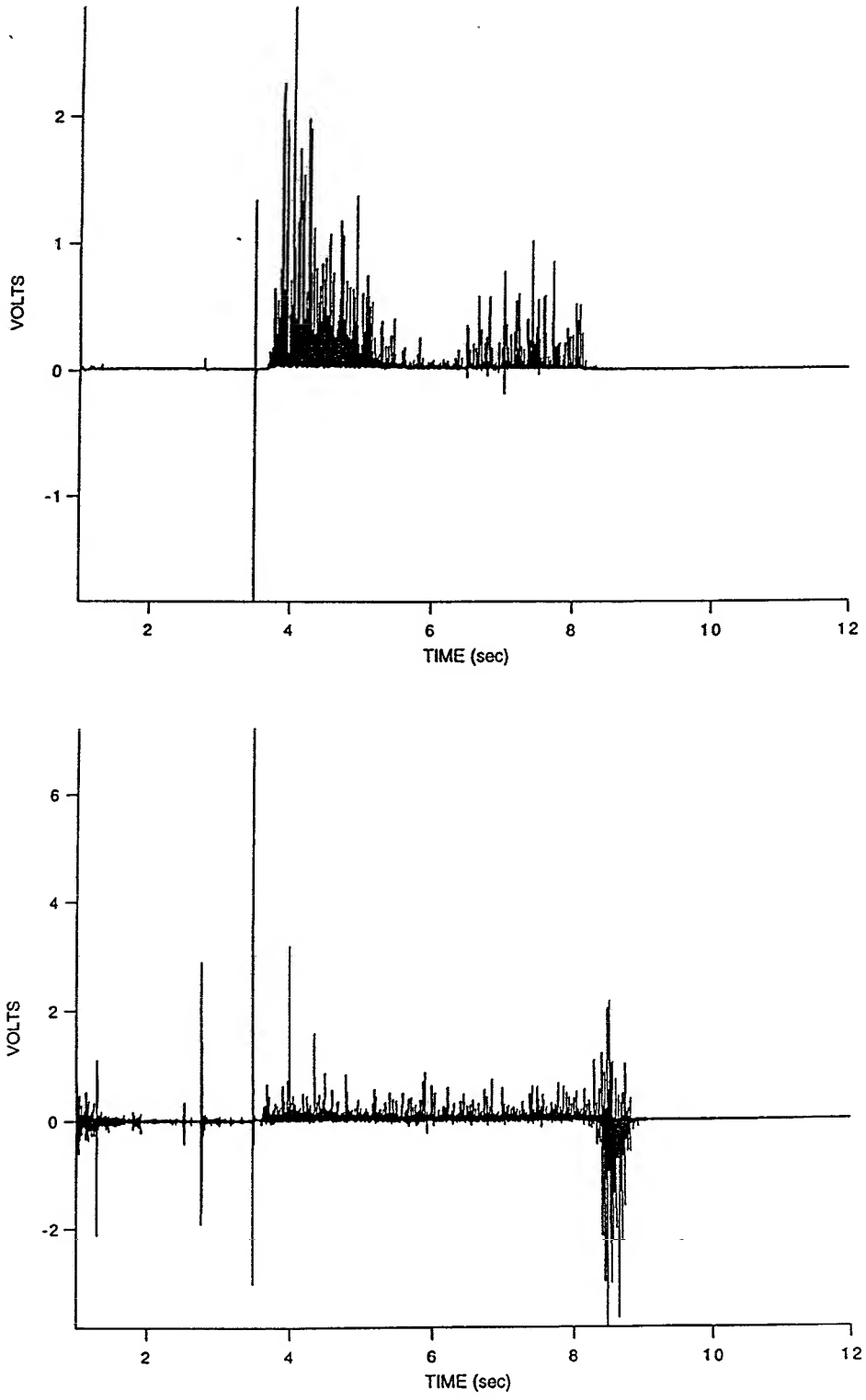

Fig. 13 A stainless strip is embedded in this cylindrical grain. There is a significantly reduced response by the probe in the top graph when compared to Figure 6. This is probably due to the reduced oxygen flow rate of 0.04 lb/sec used in this run. The bottom graph does not show a clearly discernible transition into the stainless steel. A visual inspection of the stainless steel showed some scorching of the surface but almost no ablation.

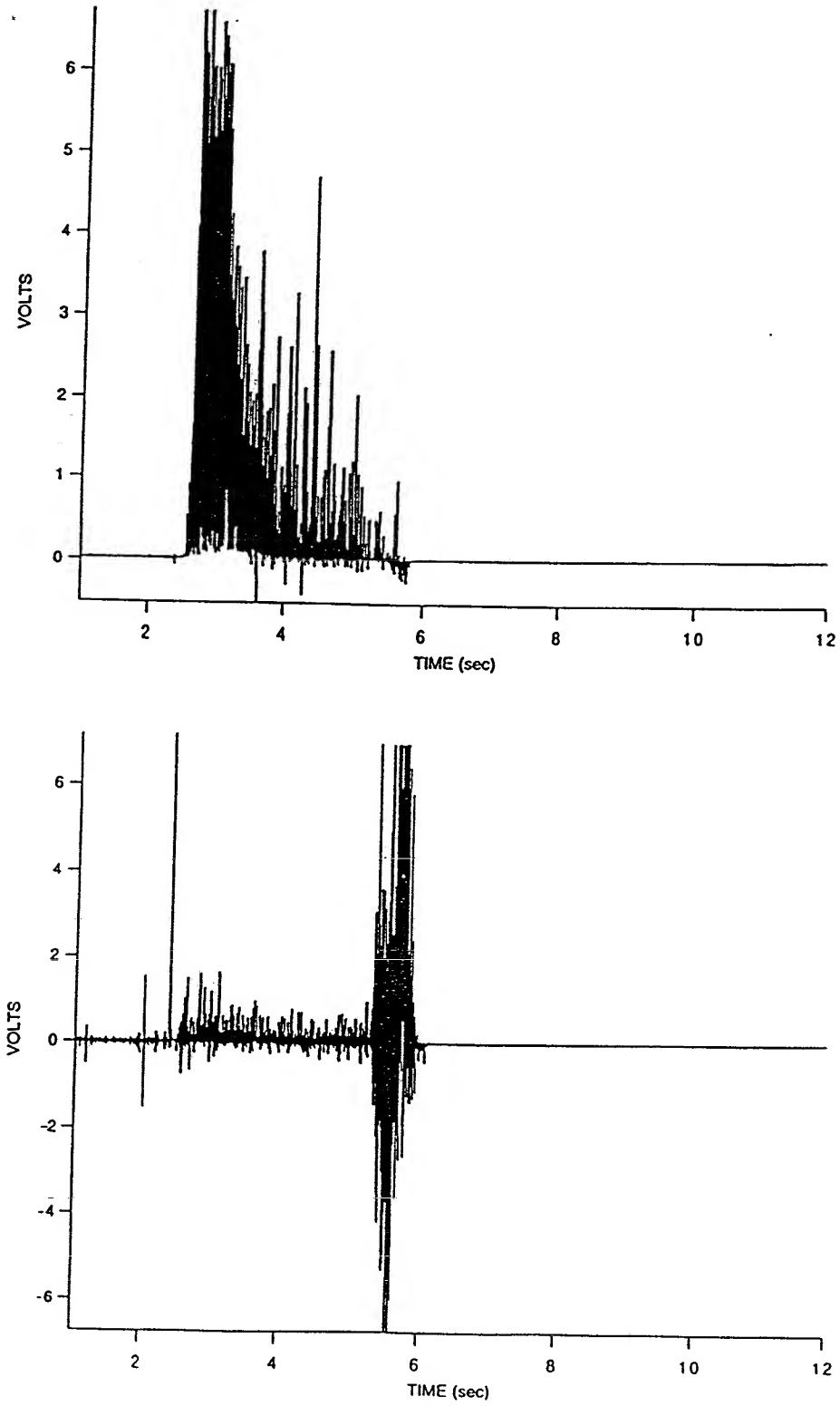

Fig. 14 This cylindrical grain shows a burn into HTPB. The initial signals are the response to the igniter wire and residual coating of the nozzle. The cylinders in the bottom graph are showing a minimal response. This run of straight HTPB is included to provide a comparison for Figure 15 which has graphite mixed with the HTPB.

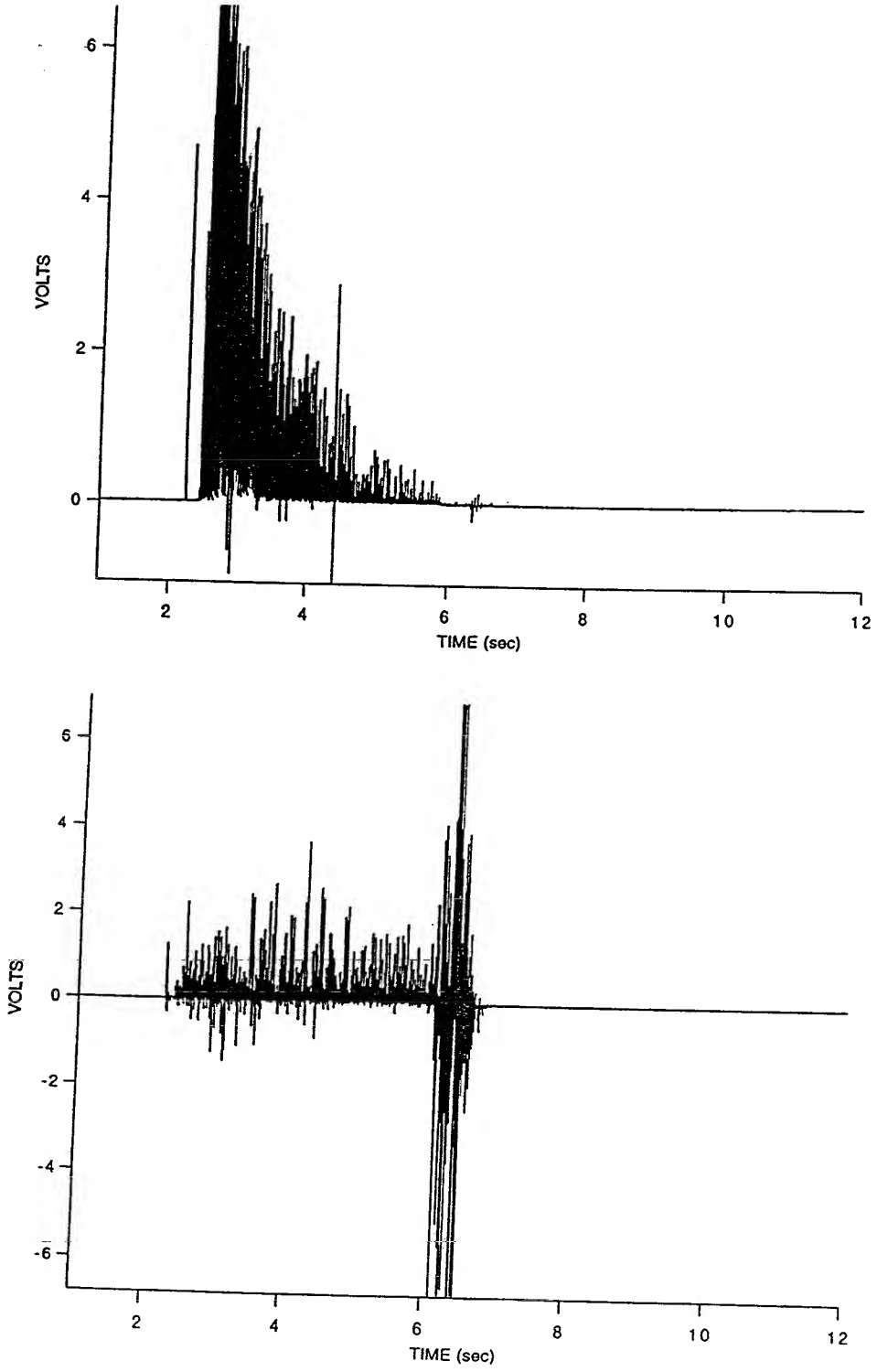

Fig. 15 This cylindrical grain has HTPB mixed with graphite in a 99 to 1 mass ratio. Comparing the probe response in the top graph with Figure 14 shows essentially the same response to the igniter wire and residual material. The Gaussian cylinders in the bottom graph have a greater response than in Figure 14. Burning the graphite apparently creates additional positive ions as shown by the bottom graph. These ions presumably do not reach the probe. The probe due to its location responds primarily to particulates. The bottom graph again shows the cylinder's response to the nitrogen purge.

REPORT DOCUMENTATION PAGE

Form Approved
OMB No. 0704-0188

1. AGENCY USE ONLY (*Leave blank*)	2. REPORT DATE	3. REPORT TYPE AND DATES COVERED
	January 5, 1998	Final Contractor Report

4. TITLE AND SUBTITLE
Detection of Metallic Compounds in Rocket Plumes Using Ion Probes

5. FUNDING NUMBERS
NAG 13-40

6. AUTHOR(S)
Robert W. Dunn

7. PERFORMING ORGANIZATION NAME(S) AND ADDRESS(ES)
Hendrix College
Department of Physics
Conway, AR 72032-3080

8. PERFORMING ORGANIZATION REPORT NUMBER

9. SPONSORING/MONITORING AGENCY NAME(S) AND ADDRESS(ES)
National Aeronautics and Space Administration
Washington, DC 20546-0001

10. SPONSORING/MONITORING AGENCY REPORT NUMBER
SE-1998-01-00001-SSC

11. SUPPLEMENTARY NOTES

12a. DISTRIBUTION/AVAILABILITY STATEMENT
Subject Category: Distribution:
Availability: NASA CASI (301) 621-0390

12b. DISTRIBUTION CODE

13. ABSTRACT (*Maximum 200 words*)

This grant experimentally verified that ion probes can consistently detect metallic compounds in a hybrid rocket plume. Two electrostatic detection methods were tested. The first method used an unbiased ion probe. It responded to collisions or near collisions with charged particulates. The amplitude of the response to metallic ions always exceeded that of the combustion products. The second device was a cylindrical Gaussian surface that surrounded, but did not touch, the plume. A charge imbalance in the plume induced a current in cylinder that was detected by a sensitive amplifier. The probe was more sensitive to metallic compounds than the cylinder. However, the Gaussian cylinder demonstrated sufficient sensitivity to warrant serious future consideration. Since the cylinder is nonintrusive, it is particularly attractive. Apparently, ions formed during combustion transfer to the metallic impurities. The formation of these metallic ions slows the ion recombination rate and helps preserve charges in the plume. The electrostatic detectors, in turn, respond to the charges carried by the metallic impurities.

14. SUBJECT TERMS	15. NUMBER OF PAGES
ROCKET PLUMES, PLUME DIAGNOSTICS	28
	16. PRICE CODE

17. SECURITY CLASSIFICATION OF REPORT	18. SECURITY CLASSIFICATION OF THIS PAGE	19. SECURITY CLASSIFICATION OF ABSTRACT	20. LIMITATION OF ABSTRACT
UNCLASSIFIED	UNCLASSIFIED	UNCLASSIFIED	UL